Seismic velocities of major silicate and oxide phases of the lower mantle

Bijaya B. Karki

Department of Chemical Engineering and Materials Science, Minnesota Supercomputing Institute
University of Minnesota-Twin Cities, Minneapolis

Lars Stixrude

Department of Geological Sciences, University of Michigan, Ann Arbor

Abstract. We have recently investigated the elastic properties of five compounds generally considered as potential consituents of the Earth's lower mantle. Full elastic constant tensors of $MgSiO_3$ and $CaSiO_3$ perovskites, MgO, CaO, and SiO_2 have been determined as a function of pressure up to 140 GPa and at zero temperature using the first principles plane wave pseudopotential method within the local density approximation. We report comprehensive comparisons of the calculated high-pressure elastic wave velocities of these phases with seismically derived lower mantle properties. The effects of iron and temperature are estimated in the case of Mg-silicate perovskite based on available experimental data. Comparison of the P and S wave velocity profiles of perovskite along a series of high-temperature isotherms to the lower mantle supports the view that this region is primarily composed of Mg-rich silicate perovskite. Our study also suggests that among the candidate phases usually considered, none are invisible. Minor phases which may be present, including magnesiowüstite, $CaSiO_3$ perovskite, and the high-pressure polymorphs of SiO_2 and CaO, have elastic wave velocities that differ significantly from those of Mg-rich silicate perovskite and may be detectable seismically.

1. Introduction

The lower mantle (670-2890 km depth) is the largest single region of the Earth's interior making up 55% of its volume. As such, it dominates the processes of mass, momentum, and energy transport in the deep interior and hence may have a substantial influence on the planet's thermal and chemical evolution. Despite a number of analyses made over several years, the major element composition of the lower mantle is still a source of controversy. Until the existence of samples from the lower mantle can be confirmed, comparison between seismological observations and the elastic properties of potentially relevant minerals and mineral assemblages represents the most direct way of extracting information regarding the composition and mineralogy of this region. Such comparisons are severely hindered by the present lack of sufficient and reliable elasticity data for the relevant phases. The majority of the measurements so far are confined to low pressures so that extrapolations to the extreme conditions corresponding to the lower mantle are needed. Alternatively, the seismic data can be extrapolated to ambient conditions for comparison with laboratory-based mineral properties. These approaches are usually based on a limited subset of seismic observations such as the density and seismic parameter (or bulk modulus), which are usually known from static compression, shock wave, and ultrasonic experiments.

First principles theory is a complementary approach that has taken on increased significance in recent years in exploration of the properties of Earth materials under extreme conditions such as those of the lower mantle (23–135 GPa). Recent advances in theory and computation have made it possible to solve the fundamental equations of quantum mechanics for large and complex systems with minimal approximation. These elaborate electronic structure calculations are completely independent of experiment and are much more reliable than traditional atomistic calculations which are based on interatomic potentials (usually parametrized from existing experimental information). One of the most accurate first principles methods currently applicable to a wide variety of materials in studying a wide range of properties is the plane wave pseudopotential approach within the framework of density functional theory [*Payne et al.*, 1992]. This method has been used in the high-pressure studies described in this paper.

We focus on two central issues regarding the composition of the lower mantle: its dominant mineralogy and the detectability of secondary and minor phases. It is generally accepted that the Earth's lower mantle is composed of an assemblage of oxides and silicates dominated by Mg-rich silicate perovskite. This view encompasses essentially all current models of lower mantle composition including those that are similar to pyrolite and those that are more rich in iron or silica [Jeanloz and Knittle, 1989; Bukowinski and Wolf, 1990; Stixrude et al., 1992; Wang et al., 1994; Zhao and Anderson, 1994]. Perovskite-rich compositions are known to agree reasonably well with the seismologically constrained density and bulk sound velocity of the lower mantle. Important uncertainties remain however, since tests against seismically observed P and S wave velocities have not been performed. The reason is that until recently, we have had no information on the shear modulus of lower mantle phases at the relevant pressures. At the same time, there is considerable interest in the detection of secondary phases in the lower mantle. Magnesiowüstite is the most commonly considered, but Ca silicate perovskite, CaO, and silica, among others, are also candidates. Of these, Ca silicate perovskite has been claimed to be an "invisible" phase because its density is similar to that of the lower mantle [Mao et al., 1989]. Again, this picture is limited because it is based on a small subset of the available seismological information and does not consider those properties of the lower mantle that are most directly determined, the velocities of P and S waves.

We have recently investigated the high-pressure (0 to 140 GPa, at 0 K) structure and elasticity of the major silicate (MgSiO$_3$ and CaSiO$_3$ perovskites) and oxide (MgO, CaO and SiO$_2$) candidate constituents of the lower mantle, using the first principles plane wave pseudopotential method [Karki et al., 1997a, b, c; Karki and Crain, 1998a, b]. In this paper we study in detail the geophysical implications of the predicted high-pressure elastic properties for the lower mantle by comparing the calculated longitudinal and shear wave velocities of these silicates and oxides and their assemblages with the seismologically derived wave velocities for this region of the Earth.

2. Computational Methods

Computations are performed using Cambridge Serial Total Energy Package (CASTEP) and Cambridge Edinburgh Total Energy Package (CETEP) codes, based on the density functional theory (DFT) under two essential approximations [Payne et al., 1992]. First, we use the local density approximation to the exchange-correlation potential (parametrization of Perdew and Zunger [1981]). Second, we use the pseudopotential approximation to represent the effective potential seen by the valence electrons due to the nucleus and frozen core electrons. The optimized, norm-conserving, non-

local pseudopotentials are generated by the Q_C-tuning method [Lee, 1995]. Structural optimization is done according to the variable cell shape molecular dynamics scheme [Wentzcovitch et al., 1993]. The calculations are well converged with respect to computational parameters such as the plane wave energy cutoff and number of special k points used; further details have been presented by Karki et al., [1997a, b, c] and Karki and Crain, [1998a, b].

We first optimize the lattice constant and internal structural parameters of a given structure at several pressures. The elastic constants are then determined from computation of the stresses generated by small deformations (strains) of the equilibrium unit cell. The ionic positions are reoptimized in the strained lattice to account for any coupling between strain and vibrational modes. We apply strains of different magnitudes and derive the elastic constants in the appropriate limit of zero strain.

3. High-Pressure Behavior of Structure and Elasticity

The predicted structure and equation of state of MgSiO$_3$ perovskite are in excellent agreement with experiment [Karki et al., 1997b]. As observed in the laboratory, we find that the structure remains orthorhombic throughout the pressure regime of the lower mantle [Knittle and Jeanloz, 1987; Funamori et al., 1996]. The calculated equation of state of CaSiO$_3$ in the cubic perovskite structure [Karki and Crain, 1998a] agrees well with the measured equation of state at lower mantle pressures [Mao et al., 1989; Wang et al., 1996]. A slight noncubic distortion in CaSiO$_3$ perovskite has been predicted by first principles linear response calculations [Stixrude et al., 1996]. The magnitude of the predicted distortion is very small, possibly too small to have been detected experimentally, and is not expected to substantially affect the elastic properties of this phase [Karki and Crain, 1998a].

The calculated equations of state of Mg, Ca, and Si oxides are in excellent agreement with experiment [Karki et al., 1997a; Karki and Crain, 1998b; Karki et al., 1997c]. MgO is found to be stable in the NaCl structure (B1 phase) up to 450 GPa and then transforms to the B2 phase (CsCl structure) [Karki et al., 1997a]. The predicted B1-B2 phase transition pressure is comparable to the all-electron linearized augmented plane wave (LAPW) prediction of 510 GPa [Mehl et al., 1988]. In the case of CaO the B1-B2 phase transition is found to occur at the much lower pressure of 58 GPa [Karki and Crain, 1998b], which falls within the experimental range of 54-70 GPa [Richet et al., 1988] and also agrees with the LAPW result of 54 GPa [Mehl et al., 1988]. Silica is predicted to transform from stishovite to the orthorhombic CaCl$_2$-type stucture at 47 GPa, in excellent agreement with the the original LAPW prediction of 45 GPa [Cohen, 1992] and the subsequent

experimentally measured value of 50 ± 3 GPa [*Kingma et al.*, 1995]. The $CaCl_2$ structure is then predicted to transform to the columbite structure (*Pbcn*) at 98 GPa, and finally to the pyrite structure at 226 GPa [*Karki et al.*, 1997c].

Full elastic constant tensors (c_{ij}) of the silicate and oxide phases are calculated from zero pressure to lower mantle pressures (up to 140 GPa) [*Karki et al.*, 1997a, b, c; *Karki and Crain*, 1998a, b]. As shown in Table 1, the calculated athermal (0 K) elastic constants at zero pressure are in excellent agreement with experimental data at ambient conditions. Effects of the zero-point motion and temperature difference between the static calculations and room temperature experiments are expected to decrease slightly the calculated values of the elastic coefficients. As expected, our results at zero pressure show better agreement with measurements than previous theoretical results based on semiempirical rigid ion

or ab initio modified electron gas or potential-induced breathing models [see *Karki et al.*, 1997a,b].

The elastic constants of all the systems studied are shown to vary strongly with pressure, particularly in the vicinity of structural transformations. Experimental measurements of the elastic constants are restricted to relatively low pressures. Our theoretical results agree well with the initial pressure dependencies of the elastic constants as determined experimentally (up to 3 GPa) for MgO and CaO [*Jackson and Niesler*, 1982; *Chang and Graham*, 1977]. In the case of $MgSiO_3$ perovskite the calculated zero pressure derivative of the shear modulus, $G' = 1.65\pm0.05$, compares favorably with the value of 1.8 ± 0.4 from recent ultrasonic interferometric data up to 8 GPa [*Sinelnikov et al.*, 1998]; however, the pressure dependencies of the individual elastic constants are still unmeasured. The observed good agreement of our theoretical prediction with the existing measure-

Table 1. Calculated Athermal Elastic (M) Moduli and Their Pressure Derivatives (M') at Zero Pressure for the Silicate and Oxides Studied in Comparison With Experiments

		c_{11}	c_{22}	c_{33}	c_{44}	c_{55}	c_{66}	c_{12}	c_{13}	c_{23}	K	G
				$MgSiO_3$ perovskite								
	Calc M	493	523	460	201	183	174	135	145	158	260	174
	M'	5.15	6.56	6.70	1.98	1.44	1.91	3.33	2.55	2.73	4.02	1.65
(1)	Exp M	482	537	485	204	186	147	144	147	146	264	177
	M'										4.0	1.8
				$CaSiO_3$ perovskite								
	Calc M	374			225			167			236	165
	M'	7.28			2.47			3.0			4.42	2.46
(2)	Exp M										232	
	M'										4.8	
						MgO						
	Calc M	291			135			90			157	120
	M'	9.0			1.30			1.91			4.27	2.39
(3)	Exp M	297			156			95			162	131
	M'	9.17			1.11			1.61			4.13	2.53
						CaO						
	Calc M	241			77			52			115	83
	M'	10.11			0.45			1.67			4.48	1.78
(4)	Exp M	223			81			59			114	81
	M'	8.7			0.74			1.71			4.05	1.81
					Stishovite							
	Calc M	456		734	254		325	216	195		310	223
	M'			4.31	2.09		3.30		2.03		4.24	1.72
(5)	Exp M	453		776	252		302	211	203		312	226
	M'										4.3	

Moduli are in GPa. 1, Experimental data are from *Yeganeh-Haeri* [1994], *Mao et al.* [1991], and *Sinelnikov et al.* [1998]; 2, from *Wang et al.* [1996]; 3, from *Jackson and Niesler* [1982]; 4, from *Chang and Graham* [1977]; 5, from *Weidner et al.* [1982] and *Andrault et al.* [1998]. Third-order Eulerian finite strain equations are fit to the calculated results except for c_{33} and c_{13} of stishovite, for which we use fourth-order fits (with $M''=0.028$ and 0.011 GPa^{-1}, respectively), and c_{11} and c_{12} of stishovite, which can be described by $(c_{11} + c_{12})/2 = 336 + 5.32P$ and $(c_{11} + c_{12})/2 = 120[1 - (P/47)^{3.5}]$, where P is the pressure in GPa.
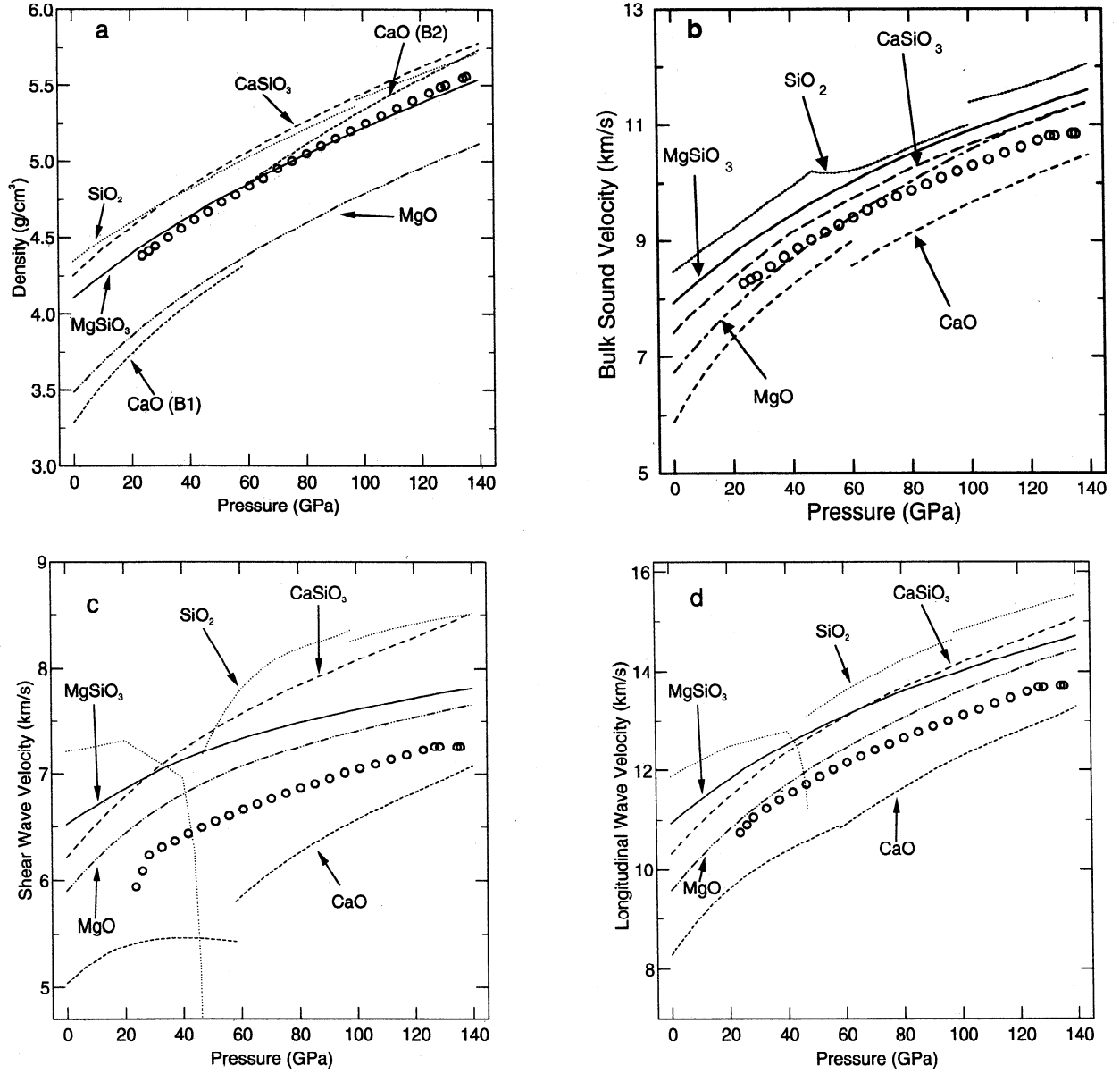
Figure 1. Comparisons of the calculated high pressure properties of silicate perovskites and oxides with the seismic properties (symbols) of the PREM lower mantle [Dziewonski and Anderson, 1981]: (a) density, (b) bulk sound velocity, (c) shear wave velocity, and (d) longitudinal wave velocity.

ments of elastic properties in the low-pressure regime and of the equation of state and phase stability over the pressure regime of the mantle gives us confidence in our theoretical predictions at geophysically relevant pressures.

4. Comparison With the Lower Mantle

4.1. Elastic Wave Velocities at High Pressure

The longitudinal (V_P) and shear (V_S) wave velocities of isotropic aggregates are given by

$$V_P = \sqrt{\frac{K + \frac{4}{3}G}{\rho}}; \qquad V_S = \sqrt{\frac{G}{\rho}} \qquad (1)$$

where ρ is the density and K and G are the isotropic bulk and shear moduli which are determined from the single-crystal elastic constants (c_{ij}) using the Hashin-Strikman averaging scheme [Watt, 1979]. The bulk sound velocity is given by

$$V_B = \sqrt{\frac{K}{\rho}} = \sqrt{V_P^2 - \frac{4}{3}V_S^2}. \qquad (2)$$

In Figure 1 we compare the calculated density, and bulk sound, longitudinal, and shear velocities of $MgSiO_3$, $CaSiO_3$, MgO, CaO, and SiO_2 with the spherically averaged (radial) seismic structure of the lower mantle taken from preliminary reference Earth model (PREM) [Dziewonski and Anderson, 1981].

The zero temperature density of $MgSiO_3$ perovskite is similar to that of the lower mantle throughout its pressure regime, whereas its velocities (V_B, V_P, and V_S) are significantly higher than the corresponding seismic profiles. The properties of perovskite in the mantle will be modified by the effects of temperature and iron content. Temperature is expected to lower the density and seismic wave velocities, while addition of Fe will increase the density and decrease the seismic wave velocities. These effects are considered in detail in section 4.2 and 4.3.

The athermal density and elastic wave velocities of MgO are all lower than those of $MgSiO_3$ perovskite. The difference in density is ~10% while the difference in elastic wave velocities is 3-5% at mid lower mantle depths. When the effects of iron are considered, the difference in density between these two minerals will decrease, and the difference in elastic wave velocities will increase. The effect of iron is explored in more detail in section 5.

The density of $CaSiO_3$ perovskite is higher than that of $MgSiO_3$ perovskite, whereas its bulk sound velocity is lower. The addition of 10% iron to $MgSiO_3$ perovskite would make its density and bulk sound velocity profiles nearly identical with those of $CaSiO_3$ perovskite [Karki and Crain, 1998a]. This similarity in properties has been noticed before and has led to the suggestions that $CaSiO_3$ perovskite would be a seismically invisible component of the lower mantle [Mao et al., 1989]. However, the shear wave velocity of $CaSiO_3$ perovskite in the lower half of the lower mantle is too high to support this view. A comparison of mineralogical properties to the entire range of seismic observations including V_P and V_S should be able to detect the Ca content of the lower mantle.

For SiO_2 the density and wave velocities are much higher than those of the lower mantle throughout its pressure regime (by as much as 20% in V_S) except in the immediate vicinity of the stishovite-to-$CaCl_2$ phase transition (47 GPa, 1180 km depth). Near this phase transition both V_P and V_S show large discontinuous changes (of ~20 and 60%, respectively) which are associated with a pressure-induced shear instability. This indicates that if free silica exists in the lower mantle, it may lead to a globally observable seismic discontinuity near a depth of 1180 km [Cohen, 1992]. The discontinuities in velocity are so large that very small amounts of silica (as little as 2%) may be detectable [Karki et al., 1997c]. Finally, the elastic wave velocities of CaO in both the B1 and B2 phases are substantially lower than those inferred from seismology, thus limiting the presence of CaO to small amounts in the lower mantle.

4.2. Effect of Iron

In order to better compare our results to the structure of the lower mantle, we must account for the effects of more complex bulk composition and solid solution on the properties of Mg-rich silicate perovskite and magnesiowüstite. We focus on the effects of iron for a number of reasons: (1) Fe is expected to be more abundant than other secondary elements that may be present such as Ca, Al, Na, and others. (2) The effect of Fe on the seismic wave velocities is expected to be large as compared with the effect of other secondary elements. (3) The effects of Fe on some of the elastic properties of Mg-rich silicate perovskite and magnesiowüstite are constrained experimentally.

The effects of iron content (X_{Fe}=Fe / (Fe + Mg)) on the density and bulk modulus of $MgSiO_3$ perovskite (Figure 2) and magnesiowüstite can be estimated in a simple way. The correction to the density comes from the increased molecular mass and a slight increase in volume, and can be described for perovskite by

$$\rho(X_{Fe}) = \rho(0)(1 + 0.26X_{Fe}) \qquad (3)$$

and for magnesiowüstite [Jeanloz and Thompson, 1983] by

$$\rho(X_{Fe}) = \rho(0)(1 + 0.76X_{Fe}). \qquad (4)$$

The bulk modulus is negligibly affected by Fe content as experiments have shown [Mao et al., 1991; Fei et al., 1992]. Because there are currently no constraints on the effect of Fe on the shear modulus of perovskite, we explore a range of models. The simplest, and most conservative, assumption is that, as in the case of the bulk modulus, Fe has only a negligible effect on the shear modulus. This assumption is not likely to be correct in detail but is useful for illustrative purposes as a probable upper bound on the shear modulus of Mg-rich silicate perovskite in the lower mantle. We also consider the possibility that the effect of Fe on the shear modulus is similar to that observed in orthopyroxene [Duffy and Anderson 1989], which can be described by

$$G(X_{Fe}) = G(0)(1 - 0.31X_{Fe}). \qquad (5)$$

Finally, we consider, as a probable lower bound on the shear modulus of Mg,Fe-silicate perovskite, that the effect of iron is the same as that observed for magnesiowüstite, which according to Duffy and Anderson [1989] can be described by

$$G(X_{Fe}) = G(0)(1 - 0.59X_{Fe}). \qquad (6)$$

4.3. Effect of Temperature

The first principles calculation of the temperature dependence of the elastic constants is possible in principle but very challenging and has not yet been performed. We may semiempirically correct our static P and S wave velocities perovskite to mantle temperatures (Figure 3) using

$$V_S(T) = V_S(0) \exp\left[\frac{\alpha T}{2}(1 - \Gamma)\right] \qquad (7)$$
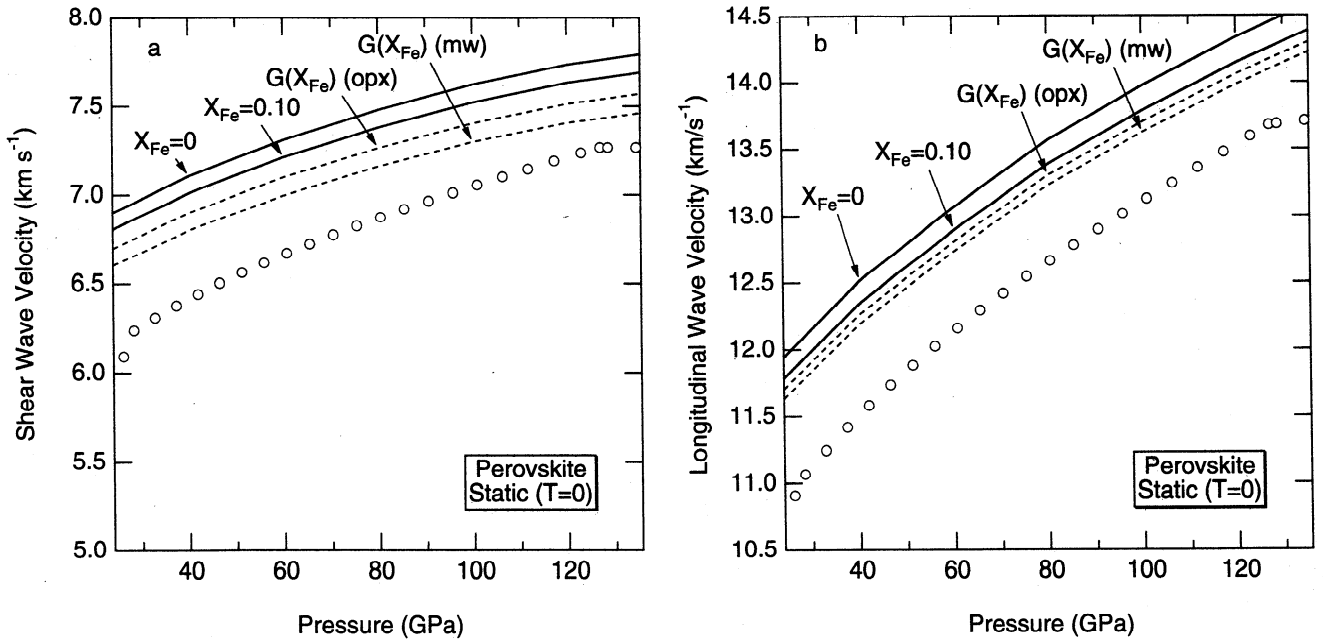
Figure 2. Estimate of the effect of iron on (a) shear and (b) longitudinal wave velocity of Mg-rich silicate perovskite under static (zero temperature) conditions. The bulk modulus is assumed unaffected by X_{Fe}, density is corrected according to Equation (3). Curves from top to bottom represent results for the pure Mg end-member and three different estimates for the effect of iron on the shear modulus of perovskite: no effect, the same effect as observed in orthopyroxene (opx) (Equation 5) and the same effect as observed in magnesiowüstite (mw) (Equation 6). Symbols are PREM data [Dziewonski and Anderson, 1981].

$$V_P(T) = V_P(0) \exp \left\{ \frac{\alpha T}{2} \left[1 - a^2 \delta_S - \frac{4}{3} b^2 \Gamma \right] \right\}, \quad (8)$$

where

$$a = \frac{V_B(0)}{V_P(0)} \quad \text{and} \quad b = \frac{V_S(0)}{V_P(0)}. \quad (9)$$

Here quantities evaluated at zero temperature are taken from our first principles calculations and the thermal expansivity α and the Anderson-Grüneisen parameters

$$\delta_S = -\frac{1}{\alpha K_S} \left(\frac{\partial K_S}{\partial T} \right)_P \quad (10)$$

$$\Gamma = -\frac{1}{\alpha G} \left(\frac{\partial G}{\partial T} \right)_P \quad (11)$$

are average values over the temperature interval [Anderson, 1995]. None of the thermal parameters are known at conditions representative of the bulk of the lower mantle; they must be estimated on the basis of partial experimental information.

The parameters that we have adopted for perovskite are summarized in Table 2 The dependence of α on pressure (density) may be described by

$$\alpha = \alpha_0 \exp \left\{ \frac{\delta_{T0}}{\kappa} \left[\left(\frac{\rho}{\rho_0} \right)^{-\kappa} - 1 \right] \right\}. \quad (12)$$

where subscript zero indicates values at ambient pressure, δ_T is the isothermal analog of δ_S, and $\kappa \approx 1.5$

[Anderson and Masuda, 1994]. Experiments on different compositions have yielded significantly different results for α_0 and δ_{T0}. We adopt values that represent experimental data for $MgSiO_3$ composition [Wang et al., 1994]

$$\alpha_0 \approx 2.4 \times 10^{-5} \text{K}^{-1} \qquad \delta_{T0} \approx 4.3. \quad (13)$$

Results for $Mg_{0.9}Fe_{0.1}SiO_3$ yield much higher values [Knittle et al., 1986; Stixrude et al., 1992]

$$\alpha_0 \approx 4.2 \times 10^{-5} \text{K}^{-1} \qquad \delta_{T0} \approx 7.0. \quad (14)$$

The reason for the differences between these two sets of results is not known, although it has been suggested that results on Fe-bearing samples are significantly biased by metastability [Bina, 1995]. Despite these differences, extrapolations based on (12) yield similar values for the thermal expansivity at conditions representative of the lower mantle: the two sets of parameters give values of α that differ by 40% at 20 GPa but only 8% at 80 GPa and 10 % at 136 GPa. As a result, the uncertainties in our thermal corrections to the seismic wave velocities are due primarily to uncertainties in Γ and δ_S.

The temperature dependence of the shear modulus is estimated on the basis of recent measurements to 8 GPa and 800 K [Sinelnikov et al., 1998]. There is some theoretical evidence that Γ decreases with increasing pressure and increases with increasing temperature [Isaak
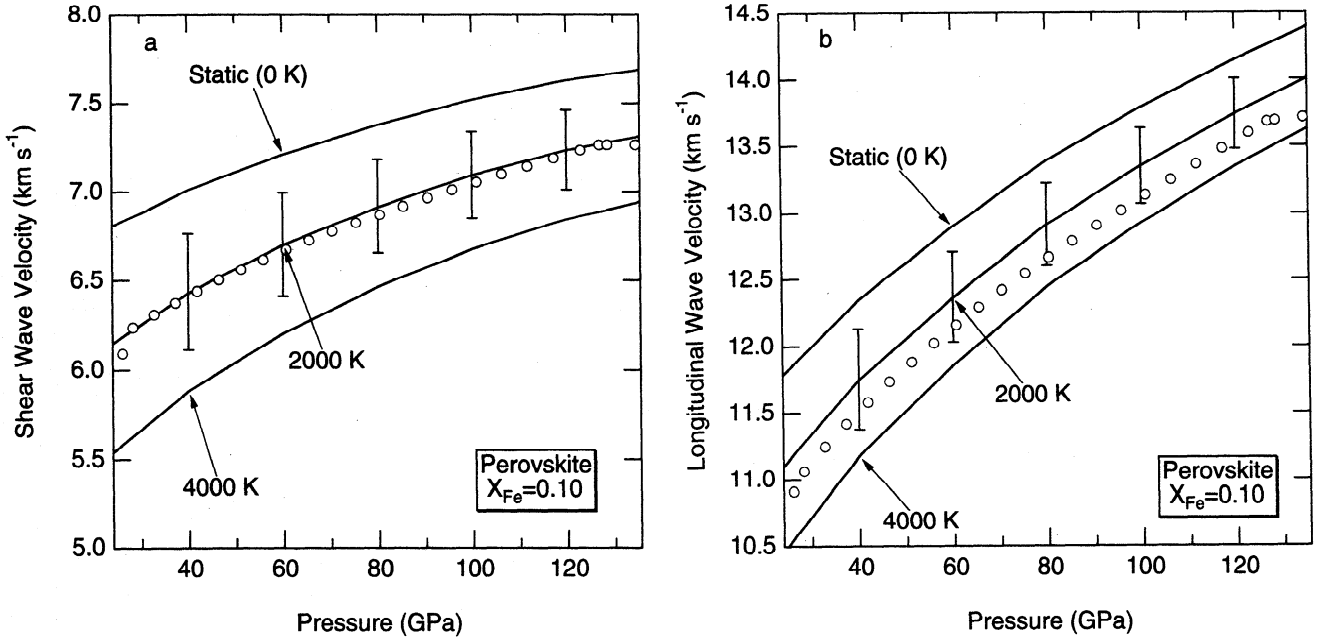
Figure 3. Estimate of the effect of temperature on (a) shear and (b) longitudinal wave velocity of $(Mg_{0.9}Fe_{0.1})SiO_3$ perovskite along three different isotherms. Error bars represent the effect of 50% uncertainty in the assumed values of Γ and δ_S. Symbols are PREM data [Dziewonski and Anderson, 1981].

et al., 1992]. Our adopted value is calculated from the measured values of G and $(\partial G/\partial T)_P$, $\alpha_0 = 2.4 \times 10^{-5}$ K^{-1} and the assignment of generous ($\pm 50\%$) uncertainties to account for the possible effects of pressure and temperature. We note that the range adopted is consistent with Birch's law of corresponding states. This approximation, under which the shear modulus is assumed to depend only on volume (no purely anharmonic thermal effects), is expected to yield a lower bound for the temperature dependence of the shear modulus

$$\Gamma > \Gamma_{cs} = \frac{K_T}{G}\left(\frac{\partial G}{\partial P}\right)_T = 2.6, \qquad (15)$$

where the subscript cs indicates the corresponding states result which is calculated from the experimental data [*Sinelnikov et al.*, 1998].

There are no experimental constraints on the temperature dependence of the adiabatic bulk modulus. The parameter δ_S is expected to decrease with increasing pressure. Theoretical calculations for MgO indicate that a value of $\delta_S \approx 1.8$ is typical of lower mantle pressures for this material [*Isaak et al.*, 1992]. The value for perovskite may be larger because δ_T of perovskite is larger than that of MgO [*Agnon and Bukowinski*, 1990; *Isaak et al.*, 1992]. The value we have adopted (2.5 ± 1.3) as being representative of perovskite for the bulk of the lower mantle is consistent within broad uncertainties with the thermodynamic expectation that $\delta_S \approx \delta_T - \gamma$ at temperatures above the Debye temperature, where γ is the Grüneisen parameter [*Anderson*, 1995].

5. Discussion

The predicted elastic wave velocities of Mg silicate perovskite, when corrected for the effects of iron and temperature, are consistent with those of the lower mantle (Figure 3). While the uncertainties in the thermal corrections do not allow us to make more precise statements regarding lower mantle composition on the basis of these results, the consistency is an important test of the plausibility of the perovskite-rich lower mantle hypothesis in terms of deep Earth observations.

At mid lower mantle depths, P and S wave velocities calculated along a 2000 K isotherm are 3.5% and 7% lower, respectively, than those at zero temperature. It is worth noting explicitly that the magnitude of the thermal correction is small compared with the effect of pressure. This is relevant because it means that theoretical calculations or experimental measurements at low temperature provide a good first approximation to the elastic wave velocities of minerals in the lower mantle.

The curves along the 2000 K isotherm are nearly parallel with those of the PREM model of the lower mantle and agree with the seismological values to within the uncertainty of the thermal correction. In detail, the calculated S wave velocity shows no systematic deviation from the seismological profile throughout the lower mantle, while the calculated P wave velocity lies systematically 1-2% higher than the PREM values. This difference is comparable to the uncertainty in the thermal correction. If the difference is significant, it may reflect the presence of other phases in the lower mantle. We note that average temperatures in the lower mantle

Table 2. Thermoelastic Parameters of $MgSiO_3$ Perovskite

Parameter	Value	Alternate Value
α_0, 10^{-5} K^{-1}	2.4	4.2
δ_{T0}	4.3	7.0
κ	1.5	
δ_S	2.5 ± 1.3	
Γ	6.8 ± 3.4	

will be somewhat > 2000 K and may increase systematically with depth due to adiabatic compression. This effect is small compared with the uncertainties in the thermal correction.

In addition to uncertainties in the thermal correction the effect of iron on the elastic wave velocities of Mg-rich silicate perovskite is also uncertain (Figure 2). We note that the P and S wave velocities shown in Figure 3 may be upper bounds as we have assumed that the shear modulus is not effected by iron content. Alternative estimates of the effect of iron yield P and S wave velocities of iron-bearing perovskite that are 1-3% lower.

While the elastic properties of Mg-rich silicate perovskite are very similar to those of the lower mantle, other candidate minerals have seismic wave velocities that differ significantly. This means that these minerals, which may be present in secondary or minor amounts, may be detectable on the basis of seismic observations and improved knowledge of their high-temperature elasticity.

Other phases that may exist in the lower mantle include magnesiowüstite, which is commonly considered as a secondary phase. The seismic wave velocities of periclase are lower than those of Mg-silicate perovskite by 3-5%. Addition of iron has a strong effect. According to Equations (4) and (6) magnesiowüstite with $X_{Fe} = 0.20$, a value appropriate for a pyrolite bulk composition, has a shear wave velocity that is 15% lower than that of $MgSiO_3$ perovskite. This large difference means that seismic wave velocities, in particular, the shear wave velocity, may be a powerful discriminant among competing compositional models of the lower mantle. At present, uncertainties in thermal and compositional corrections still prevent us from making use of this compositionally sensitive portion of the seismological data base at the level of detail that would be necessary to distinguish pyrolite from the more iron- or silica-rich compositions that have been proposed.

Minor candidate lower mantle phases, including $CaSiO_3$ perovskite, CaO and silica also have distinct elastic properties. While the density of Ca- and Mg-rich silicate perovskites are similar, the seismic wave velocities of $CaSiO_3$ perovskite are predicted to be higher: roughly 10% higher in shear wave velocity than $MgSiO_3$

perovskite near the base of the mantle. This is significant because it means that when all seismological observations are taken into account, Ca perovskite can no longer be considered an invisible component of the lower mantle. Silica also has very distinctive seismic wave velocities, in particular, in the vicinity of the pressure-induced shear instability and phase transition near 47 GPa. The velocity contrast across this transition is so large that as little as few percent silica may be detectable in the lower mantle, possibly as a seismically reflective feature near 1180 km depth [*Karki et al.*, 1997c].

6. Conclusion

We have predicted from first principles theory the elastic wave velocities of major lower mantle consituents at geophysically relevant pressures (0 to 140 GPa at 0 K). Comparison of the athermal theoretical results with lower mantle properties supports the prevailing view that the lower mantle consists primarily of Mg-rich silicate perovskite. Detailed consideration of the effects of temperature and iron content on the elasticity of this phase, based on semiempirical correction of our theoretical results, further supports the perovskite-rich lower mantle hypothesis. Uncertainties in the semiempirical thermal and compositional corrections do not yet permit more precise statements regarding lower mantle composition on the basis of the P and S wave velocities of this region. Our results on other candidate lower mantle phases indicate that as the thermoelastic properties of Mg-rich silicate perovskite at lower mantle conditions become better constrained, it should be possible to detect a number of minor or secondary phases in the lower mantle: magnesiowüstite, $CaSiO_3$ perovskite, and silica all have distinctive seismic wave velocities. Further progress should include experimental tests of our predicted high-pressure elastic wave velocities and better experimental and theoretical constraints on the effect of temperature and iron.

References

Agnon, A., and M. S. T. Bukowinski, Thermodynamic and elastic properties of a many-body model for simple oxides, *Phys. Rev. B Condens. Matter, 41*, 7755-7766, 1990.

Anderson, O. L., *Equations of State of Solids for Geophysics and Ceramic Science*, Oxford Univ. Press., New York, 1995.

Anderson, O. L., and K. Masuda, A thermodynamic method for computing thermal expansivity, α, versus T along isobars for silicate perovskite, *Phys. Earth Planet. Inter., 85*, 227-236, 1994.

Andrault D., G. Fiquet, F. Guyot, and M. Hanfland,

Pressure-induced landau-type transition in stishovite. *Science, 282*, 720-724, 1998.

Bina, C. R., Confidence limits for silicate perovskite equations of state, *Phys. Chem. Miner., 22*, 375-382, 1995.

Bukowinski, M. S. T., and G. H. Wolf, Thermodynamically consistent decompression: Implications for the lower mantle composition, *J. Geophys. Res., 95*, 12583-12593, 1990.

Chang, P., and E. K. Graham, Elastic properties of oxides in the NaCl-structure, *J. Phys. Chem. Solids, 38*, 1355-1362, 1977.

Cohen, R. E., First-principles predictions of elasticity and phase transitions in high pressure SiO_2 and geophysical implications, in *High-Pressure Research: Applications to Earth and Planetary Sciences* edited by Y. Syono and M. H. Manghnan, pp. 425-431, Terra Sci., Tokyo, 1992.

Duffy, T. S., and D. L. Anderson, Seismic velocities in mantle minerals and the mineralogy of the upper mantle, *J. Geophys. Res., 94*, 1895-1912, 1989.

Dziewonski, A. M., and D. L. Anderson, Preliminary reference Earth model, *Phys. Earth Planet. Inter., 25*, 297-356, 1981.

Fei, Y., H. K. Mao, J. Shu, and J. Hu, P-V-T equation of state of magnesiowustite ($Mg_{0.6}Fe_{0.4}O$), *Phys. Chem. Miner., 18*, 416-422, 1992.

Funamori, T., T. Yagi, W. Utsumi, T. Kondo, T. Uchida, and M. Funamori, Thermoelastic properties of $MgSiO_3$ perovskite determined by in situ X-ray observations up to 30 GPa and 2000 K, *J. Geophys. Res., 101*, 8257-8269, 1996.

Isaak, D. G., O. L. Anderson, and R. E. Cohen, The relationship between shear and compressional velocities at high pressures: Reconciliation of seismic tomography and mineral physics, *Geophys. Res. Lett., 19*, 741-744, 1992.

Jackson, I., and H. Niesler. The elasticity of periclase to 3 GPa and some geophysical implications, in *High-Pressure Research in Geophysics* edited by S. Akimoto and M. H. Manghnani, pp. 93-133, Cent. for Acad. Pub., Tokyo, 1982.

Jeanloz, R., and E. Knittle, Density and composition of the lower mantle, *Philos. Trans. R. Soc. Ser. A, 238*, 377-389, 1989.

Jeanloz, R., and A. B. Thompson, Phase transitions and mantle discontinuities, *Rev. Geophys., 21*, 51–74, 1983.

Karki, B. B., and J. Crain, First-principles determination of elastic properties of $CaSiO_3$ perovskite at lower mantle pressures, *Geophys. Res. Lett, 25*, 2741-2744, 1998a.

Karki, B. B., and J. Crain, Structure and elasticity of CaO at high pressure, *J. Geophys. Res., 103*, 12405-12411, 1998b.

Karki, B. B., L. Stixrude, S. J. Clark, M. C. Warren, G. J. Ackland, and J. Crain, Structure and elasticity of MgO at high pressure, *Am. Mineral., 82*, 51-60, 1997a.

Karki, B. B., L. Stixrude, S. J. Clark, M. C. Warren, G. J. Ackland, and J. Crain, Elastic properties of orthorhombic $MgSiO_3$ perovskite at lower mantle pressures, *Am. Mineral., 82*, 635-638, 1997b.

Karki, B. B., L. Stixrude, and J. Crain, Ab-initio elasticity of three high-pressure polymorphs of silica, *Geophys. Res. Lett, 24*, 3269-3272, 1997c.

Kingma, M. J., R.E. Cohen, R.J. Hemley, and H.K. Mao, Transformation of stishovite to a denser phase at lower mantle pressures, *Nature, 374*, 243-245, 1995.

Knittle, E., and R. Jeanloz, Synthesis and equation of state of (Mg,Fe)SiO_3 perovskite to over 10 gigapascals, *Science, 235*, 666-670, 1987.

Knittle, E., R. Jeanloz, and G. L. Smith, Thermal expansion of silicate perovskite and stratification of the earth's mantle, *Nature, 319*, 214-216, 1986.

Lee, M. H., Advanced pseudopotentials for large scale elec-

tronic structure calculations, Ph.D. thesis, Univ. of Cambridge, Cambridge, England, 1995.

Mao, H. K., L. C. Chen, R. J. Hemley, A. P. Jephcoat, Y. Wu, and W. A. Bassett, Stability and equation of state of $CaSiO_3$ perovskite to 134 GPa, *J. Geophys. Res., 94*, 17889-17894, 1989.

Mao, H. K., R. J. Hemley, Y. Fei, J. F. Shu, L. C. Chen, A. P. Jephcoat, Y. Wu, and W. A. Bassett, Effect of pressure, temperature, and composition on lattice parameters and density of (Fe,Mg)SiO_3-perovskites to 30 GPa, *J. Geophys. Res., 96*, 8069-1079, 1991.

Mehl, M. J., R. E. Cohen, and H. Krakauer, Linearized augmented plane wave electronic structure calculations for MgO and CaO, *J. Geophys. Res., 93*, 8009-8022, 1988.

Payne, M. C., M. P. Teter, D. C. Allen, T. A. Arias, and J. D. Joannopoulos, Iterative minimisation techniques for ab initio total-energy calculations: Molecular dynamics and conjugate gradients, *Rev. Mod. Phys., 64*, 1045-1097, 1992.

Perdew, J. P., and A. Zunger, Self-interaction correction to density functional approximations for many-electron systems, *Phys. Rev. B, 23*, 5048-5079, 1981.

Richet, P., H. K. Mao and P. M. Bell, Static compression and equation of state of CaO to 1.35 Mbar, *J. Geophys. Res., 93*, 15279-15288, 1988.

Sinelnikov, Y. D., G. Chen, D. R. Neuville, M. T. Vaughan, and R. C. Liebermann, Ultrasonic shear wave velocities of $MgSiO_3$ perovskite at 8 GPa and 800 K and lower mantle composition, *Science, 281*, 677-679, 1998.

Stixrude, L., R. J. Hemley, Y. Fei, Y., and H.-K. Mao, Thermoelasticity of silicate perovskite and magnesiowüstite and the stratification of the Earth's mantle, *Science, 257*, 1099-1101, 1992.

Stixrude, L., R. E. Cohen, R. Yu, and H. Krakauer, Prediction of phase transition in $CaSiO_3$ perovskite and implications for lower mantle structure, *Am. Mineral., 81*, 1293-1296, 1996.

Wang, Y., D. J. Weidner, R. C. Liebermann, and Y. S. Zhao, P-V-T equation of state of (Mg,Fe)SiO_3 perovskite. Constraints on composition of the lower mantle, *Phys. Earth Planet. Inter., 83*, 13-40, 1994.

Wang, Y., D. J. Weidner, and F. Guyot, Thermal equation of state of CaSiO_3 perovskite, *J. Geophys. Res., 101*, 661-672, 1996.

Watt, J.P., Hashin-Shtrikman bounds on the effective elastic moduli of polycrystals with orthorhombic symmetry, *J. Appl. Phys., 50*, 6290-6295, 1979.

Weidner, D. J., J. D. Bass, A. E. Ringwood, and W. Sinclair, The single-crystal elastic moduli of stishovite, *J. Geophys. Res., 87*, 4740-4746, 1982.

Wentzcovitch, R. M., J. L. Martins, and G. D. Price, Ab initio molecular dynamics with variable cell shape: Application to $MgSiO_3$ perovskite, *Phys. Rev. Lett., 70*, 3947-3950, 1993.

Yeganeh-Haeri, A., Synthesis and re-investigation of the elastic properties of single-crystal magnesium silicate perovskite, *Phys. Earth Planet. Inter., 87*, 111-121, 1994.

Zhao, Y. S., and D. L. Anderson, Mineral physics constraints on the chemical composition of the Earth's lower mantle, *Phys. Earth Planet. Inter., 85*, 273-292, 1994.

B. B. Karki, Department of Chemical Engineering and Materials Science, University of Minnesota, 421 Washington Ave., SE, Minneapolis, MN 55455. (karki@cems.umn.edu)

L. Stixrude, Department of Geological Sciences, University of Michigan, 425 E. University Ave., Ann Arbor, MI 48109-1063. (stixrude@umich.edu)